Bi_2S_3 Nanowires Fabricated via HVPC Growth Technique for Photosensor Application

Bheim M. Llona, Gil Nonato C. Santos, Reuben V. Quiroga

Abstract- Bi_2S_3 Nanowires was successfully fabricated using Horizontal Vapor Phase Crystal growth technique for photosensor application. A 35 mg of bismuth sulfide powder with purity rate of 99.9 % was utilized. The growth temperature was varied at 600 ^oC to 1200 ^oC with growth time of 4 to 8 hours where the ramp time was set at 60 minutes. The as-prepared products were characterized using an SEM, EDX, and Applied Spectral Imaging. The optimum growth was at 1200°C deposited on zone 2 on a fused silica tube. The energy band gap was 2.58 eV which has blue spectra. The nanowires demonstrated its functionality as photosensor in a metal-semiconductor-metal planar structure based on the voltage time spectra obtained.

Keywords - Bismuth Sulfide Nanowires, Quantum Confinement Effect, Horizontal Vapor Phase Crystal (HVPC) Growth Technique, Photosensor

1 INTRODUCTION

Potential applications of nanomaterials are on the center stage of interest nowadays particularly on electronic industries where size of devices are really of concern. In the recent years, remarkable effort has been devoted for the fabrication and the characterization of the semiconductive nanomaterials from the main-group metals chalcogenides (A_2B_3 with A=Sb, Bi, As, and B=S, Se, Te) to explore their novel properties for promising application (Lu, Han, Yang, Lu, and Wang, 2007; Yu, Cao, and Zhu, 2005).

Among the semiconductive nanomaterials, Bismuth Sulfide (Bi_2S_3) has attracted great attention for its technological applications. Bi_2S_3 is a kind of layered semiconductor with orthorhombic system whose direct band gap (E_g) is 1.3 eV in bulk form, which closely lies in visible solar energy spectrum and is useful for photodiode arrays or photovoltaic conversion, IR spectroscopy, television cameras, optoelectronic devices, decorative coating, and thermoelectric devices (Chai et al., 2008; Ubale et al., 2008; Xu et al., 2010; Thongtem et al., 2010). In addition, the optoelectronic response and the surface chemical properties of the Bi_2S_3 nanowires have been studied and it demonstrated a wide wavelength applicable to optical detector/switches and sensors (Xi, Hu, Zhang, Zhang, Wang, 2009). Field-effect transistors (FETs) have also been fabricated using a single Bi_2S_3 nanowire with high on/off ratio of orders of magnitude (Yu & Sun, 2009).

Moreover, Bi_2S_3 nanorods, nanotubes, nanowires, urchin-like nanostructures, 3D snowflake-like Bi_2S_3 nanostructures, 3D flower-like superstructures, nanoflowers, and quantum-sized Bismuth(III) Sulfide particles were produced by different methods such as, for nanorods, solid state reaction route (Chai et al.,2008), microwave irradiation method (Thongtem et al., 2010), solvothermal synthesis (Zhu et al., 2008), solution-phase route (Liu et al., 2005), surfactant-assisted solvothermal method (Ma et al., 2007), and sonochemical method (Zhu et al., 2003).

Of all the nanomaterials that can be fabricated from Bi_2S_3, it is the nanowires that draw the attention of many researchers because of its claimed properties, like the quantum confinement effects and the electrical, optical and magnetic properties. A nanowire, in general, is usually referred to as a cylindrical solid wire with a diameter ranging from 10s to 100s of nanometers and a length in the order of microns. Their structure can range from crystalline to polycrystalline to nearly amorphous. This has application to biomedical engineering in the manipulation of biological cells in magnetic fields, in electronic devices including field-effect transistors (FETs), sensors, detectors, and light emitting diodes (LEDs), in chemical separation, in high–density data storage, such as magnetic read heads or patterned storage media, and electronic and opto-electronic nanodevices for metallic interconnections of quantum devices and nanodevices which allow the replacement of copper in computers and in other electronic devices (Willems & van den Wildenberg, 2004).

Stimulated by the promising application and assurance of fabricating Bi_2S_3 nanowires, this paper focused on the electronic application of Bi_2S_3 particularly for its photosensing capabilities. However, these Bi_2S_3 nanowires will be synthesized using a method different from the above-

- *Bheim M. Llona, Master of Science in Physics, De La Salle University-Manila, Philippines. E-mail: Bheim.llona@dlsu.edu.ph*
- *Gil Nonato C. Santos, Doctor of Philosophy in Materials Science, Professor, De La Salle University-Manila, Philippines. E-mail: santosg@dlsu.edu.ph*
- *Reuben V. Quiroga, Doctor of Philosophy in Physic, De La Salle University-Manila, Philippines. E-mail: quirogar@dlsu.edu.*

mentioned syntheses-strategies, which is the Horizontal Vapor Phase Crystal (HVPC) growth technique. The effect of varying the growth temperature and the growth time on the surface topography, morphology, and elemental composition will be investigated using a Scanning Electron Microscope (SEM), and Energy Dispersive X-ray (EDX). Its photoluminescence will also be explored using Applied Spectral Imaging. The focal point of the study was to determine the optimum growth conditions, to demonstrate the functionality and to verify the quantum confinement effect of the as-prepared Bi_2S_3 nanowires for photosensing applications.

2 EXPERIMENTAL DETAILS

There were two major parts in this study, namely: optimization of growth conditions, and demonstration for photosensor application. The optimization was made so that more nanowires in a desirable enough area would be produced. This was done by knowing what zone would be the nanowires would grow and at what parameters this would took placed uniformly. The growth temperature would range from 600°C, 800 °C, 1000 °C and 1200°C while the dwell time would be set at 4 hours, 6 hours, and 8 hours, and the ramp time was taken to be a constant at 60 minutes. To do this, the procedure was followed on the technique of Santos (2007). But in terms of the zonal division, the researcher had selected three zones only. After obtaining the optimum conditions, the second part of the study-the photosensor application commenced. For easy deposition of Bismuth Sulfide nanowires, the glass substrate must be in a mechanical equilibrium. So, the researcher had to modify the technique in some step in the procedure of Santos (2007) to keep the glass substrate stable. This was done by having some dent in the tube to hinder the glass substrate from sliding.

The following were the complete descriptions of the commonality and differences of both procedures:

A. Preparation of Raw Materials

Guided by the procedures found in the work of Espulgar (2010), the fused-silica tube was prepared by sealing its one end using a high temperature blow torch (mixture of LPG and oxygen). This tube had a dimension as follows: inner size diameter of 9 mm, outer size diameter of 11 mm, and length of 220 mm. By the use of an ultrasonic, the fused silica tube would be then cleansed just for 30 minutes for which afterwards would be rinsed and dried. In the present study, the material would be the Bismuth Sulfide powder (approximately 0.035 grams) of high purity (99.99%) which would be loaded into the tube. The tube with Bismuth Sulfide powder would be connected to a Thermionic High Vacuum System to decrease the pressure at around 10^{-6} Torr and would then be fully sealed and detached using the blow torch again.

For the second part, this step would be done again but unlike before, the tube would have now some dent according to where the nanowires or other nanomaterials grown and to what was intended to be deposited onto substrate. This was done to ensure that the nanowires or other nanomaterials would grow on the glass substrate placed inside the tube.

B. Growth of Bismuth Sulfide Nanomaterials

Placed halfway in horizontal orientation inside a Thermolyne furnace, the fully sealed fused-silica tube containing the Bismuth Sulfide powder would be baked there. However, before operating the furnace, it must be programmed at a ramp time of 60 minutes, at a certain growth temperature (600 °C, 800 °C, 1000 °C, 1200 °C), and at a certain growth time (4 hours, 6 hours, 8 hours) for which afterwards baking could be performed. This was done to achieve the desirable temperature gradient necessary for the growth of nanomaterials. This would also trigger the thermal diffusion of Bismuth Sulfide powder as it evaporates from the hotter end of the tube and then condense towards the colder end. After all these, the set up would be allowed to cool down naturally up to room temperature.

For the application part, the parameters were now then held fixed provided these were the optimum parameters for growing the nanowires. This would guarantee and pave the way for nanowires to grow according to what was needed in the study.

C. Bismuth Sulfide Nanomaterials Retrieval

On one hand, the cooled fused-silica tube would be fully covered by a masking tape. Afterwards, it would be sectioned into three parts by marking it with a pen. The quartz tube would then be cracked under fume hood. Fragments of the cracked quartz tube with deposits of Bismuth Sulfide nanomaterials would be subjected to characterization.

On the other hand, what was being retrieved for application was the glass substrate with nanomaterials. This can be done even without masking tape because cracking the dent part would allow us to retrieve the glass substrate with nanomaterials, undamaged.

D. Characterization

This step was true to all major parts of study. The Bismuth Sulfide deposits will be characterized using JEOL-JSM 5310 Scanning Electron Microscope (SEM), and EDX was conducted using the same equipment too. SEM would be used to determine if Bismuth Sulfide nanomaterials were present on the fragments of the quartz tube or in glass substrate and what structure or morphology formed. Using the EDX, the elemental composition would be determined completely.

For application part, the optical property characterization would be now performed for the glass-substrate-nanomaterials to ensure its functionality for photosensor application. This could be done using the Applied Spectral Imaging SD-300. In this characterization, the optical band gap of the assemblies of nanowires would be determined based on the spectra. These spectra of the samples were investigated under white light source excitation. White light source has three excitation wavelength ranges: 360-370 nm, 530-550 nm, and 460-495 nm.

E. Parametric Analysis

This step was useful for optimization of parameters to which it would give information to the best parameters for fabricating Bismuth Sulfide nanowires. For the characterized Bismuth Sulfide nanomaterials grown using the Horizontal Vapor Phase Crystal (HVPC) Growth Technique in various growth temperatures and growth time, the optimum growth conditions could be inferred. The desired zone and nanomaterials for optoelectronic nanodevices applications could therefore be synthesized efficiently.

However, this step was not going to perform again for part two because only the optimum conditions were being used for application part. In short, the optimum conditions in here would be then held fix during the investigation of the applicability of the sensor made.

F. Testing Circuit for Photosensor Characterization

In this study, to characterize the sensor made, researcher used the change in the voltage-time spectra of Bismuth Sulfide nanowires based-sensor to see the voltage responses of it to white light.

According to Ahire (2007), a photosensor is an electronic element that senses the incidence of visible light, infrared, and ultra violet ray. In the study, only the visible light would be detected by the photoconductive detector so the experimental set up for photosensor characterization would be as follows:

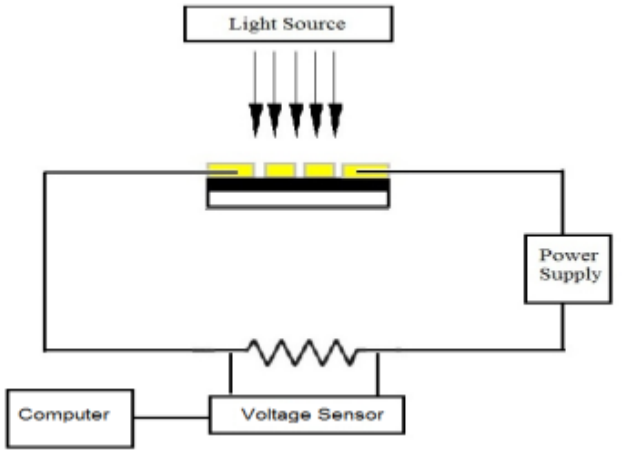

Fig.1.Testing Circuit

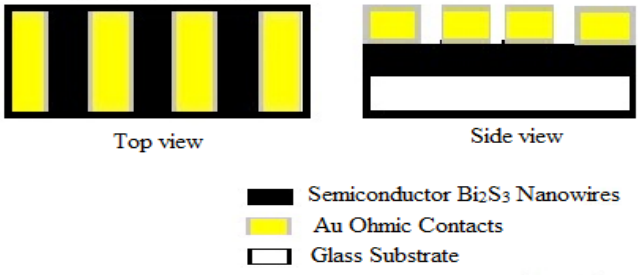

Fig. 2. Schematic Structure of photoconductive detector.

In fig. 1, Light was directed at the photoconductive detector resulted in a photoelectric effect. However in this case this effect is known to be the photoconductive effect. According to Cua et al, 1996, in the photoconductive effect light changes the electrical conductivity of a material. Moreover the material in this case was a semiconductor, thus the electrons was fixed in the valence bonds of the atoms but a few electrons with higher energies would have broken bonds and they would be free to serve as mobile charges in conduction. The energy differential needed to break a bond is called the energy gap. If the light source carries sufficient photon energy, then the absorption of light will free an electron that will take part in the conduction of the semiconductor. Hence, the action of light induces free carriers, both electrons and holes, of the sample-bismuth sulfide nanowires sensor. In the study of Ahire et al, 2007, photosensor characteristics was studied using Lab equipment unit (model no. 2004) with a 500 W tungsten filament bulb was used as light source. In the present study, this would be done using units of voltage sensor PASCU equipment with a 120 W tungsten filament bulb-light source at vertical distance of 8 cm from the sample.

Among various types of detectors (Sun et al 2010); metal-semiconductor-metal (MSM) detector, a Schottky photodiode, a p-n photodiode, and so on, the MSM structured photoconductive detectors with two ohmic contacts were generally the simplest detectors to grow and fabricate, and they were also easy to obtain higher gain and photoresponsivity. Moreover, According to Parker (1994), a photoconductive detector is not a junction detector; it's simply a slab of semiconductor with a pair of ohmic end contacts. This simple device, without any junctions, could give more current carriers to an external circuit than incoming photons. In fig.2, it shows a schematic structure of the photoconductive detector to be fabricated in this study. It consists of glass substrate, a typical microscopic glass with dimensions 9mm

x10 mm to where the Bismuth Sulfide Nanowires would be deposited. In short it served as the glass support to where the nanowires would lie on since at the moment it is impossible to manipulate the nanowires alone. Afterwards, the glass had been cut and cleansed before it placed lengthwise into a fused-silica tube with dent. It was the time for the bismuth sulfide nanowires to be deposited. After deposition of the material, it would now be subjected to a gold coating in order to have an ohmic contact. However, to do that the sample will be placed on the holder with three wires to be shadow-masked by the gold coater shot in 90 s duration of time. Fig. 3 displayed the sample holder with three wires serves as mask used in the study. As it shown, the gap between each of the electrodes could be determined by the diameter of the wire used thus, using the vernier caliper, the diameter of the wire which in effect the gap between electrodes was equal to 75 μm. The researcher used three gaps to have more area exposed to light and to ensure the device will response to light. It would then be subjected to gold coat before it would be put into the test circuit.

Fig. 3. Sample holder with three wires serves as mask.

3 RESULTS AND DISCUSSIONS

A. Part I: Optimization

In this part the Bismuth Sulfide Nanowires was investigated. Presented here were the thorough observed dominating nanowires grown in three different zones of fused silica tube as shown below. The zone 1 was the hottest part (1-4 cm), the zone 2 was the middle part (5-8 cm), and the zone 3 was the coolest part (9-12 cm) since this part was protruded outside. The in-between distances (4-5 cm and 8-9 cm) were allotted for the would-be-dent for application part

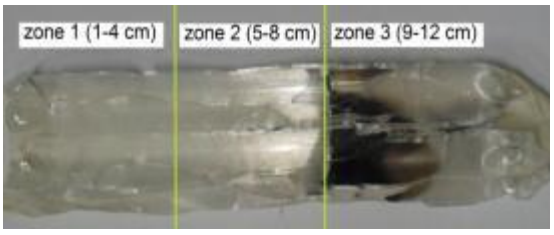

Fig. 4. Fused-Silica tube divided in three zones after the fabrication of Bi_2S_3 nanomaterials

In line with searching for the best zone in fabricating nanowires, SEM tool was utilized. For SEM micrographs (see Appendix A), it was from there the optimum parameters condition were obtained. At growth temperature 1200 ^{o}**C**, dwell time 4 hours, ramp time 60 minutes, and in zone 2, between 5 and 8 cm from the hottest region, rich bismuth sulfide nanowires with almost horizontal orientation were formed. These were considered by the researcher as the optimum parameters. Based on the pattern exhibited on the micrographs of nanomaterials, larger 3 dimensional bismuth sulfide nanostructures were fabricated in the highest temperature. On the other hand, smaller nanomaterials were synthesis in a lowest temperature. Furthermore, as the dwell time was increased the thicker the nanostructures formed. In other words, more and more nanostructures were synthesized.

Moreover, results from SEM shows the growth of semiconductor islands self-assembly growth mechanism particularly the Stranski-Krastanov growth mode which clearly seen from the micrographs the formation of the three dimensional nanostructures. Here were the summary of the nanomaterials in Table I.

TABLE I
SUMMARY OF THE NANOSTRUCTURES FABRICATED

Temp. (^{o}C)	Time (hr.)	Zone		
		1	2	3
1200	8	➢Web-like nanostructures ➢ Nanorods	➢Nanowires ➢Nanoleaves ➢Nanorods	➢Nanobamboo ➢Urchin-like nanostructures ➢Nanorods ➢Faceted nanostructures
1000	8	➢Web-like nanostructures	➢Nanospheres ➢Nanowires ➢Nanoleaves	➢Nanospheres ➢Nanoparticles
800	8	➢Nanospheres ➢Nanorods	➢Nanoleaves ➢Nanowires	➢Nanoparticles ➢Nanospheres ➢Faceted nanostructure
600	8	➢Web-like nanostructures ➢ Nanorods	➢Urchin-like nanostructures ➢Web-like nanostructures	➢Nanoflowers
1200	6	➢Web-like nanostructures ➢ Nanorods	➢Web-like nanostructures ➢ Nanorods	➢Urchin-like nanostructures ➢Nanoleaves ➢Nanobamboo
1000	6	➢Nanospheres ➢Nanorods ➢Faceted nanostructures	➢Nanorods ➢Nanowires	➢Nanospheres ➢Nanoflowers ➢Nanowires
800	6	➢Nanospheres ➢Web-like nanostructures ➢Nanowires	➢Nanorods ➢Web-like nanostructures ➢Nanowires	➢Nanospheres ➢Nanoleaves ➢Urchin-like nanostructures ➢Faceted nanostructures

600	6	➢Web-like nanostructures ➢Nanorods	➢Web-like nanostructures ➢Nanorods	➢Nanospheres ➢Web-like nanostructures ➢Nanorods ➢Faceted nanostructures
1200	4	➢Web-like nanostructures	➢Nanowires	➢Nanoleaves ➢Nanoflowers ➢Faceted nanostructures ➢Quantum dots
1000	4	➢Web-like nanostructures	➢Urchin-like nanostructures ➢Nanowires ➢Nanorods ➢Faceted nanostructures	➢Nanospheres ➢Nanowires ➢Faceted nanostructures
800	4	➢None	➢Nanobamboo ➢Nanowires ➢Nanospheres	➢Web-like nanostructures ➢Nanowires ➢Nanoparticles ➢Quantum dots
600	4	➢Faceted nanostructures ➢Web-like nanostructures	➢Nanowires ➢Nanoleaves	➢Web-like nanostructures ➢Faceted nanostructures

B. Part II: Photosensing Application

After determining of the optimum parameters for fabrication, bismuth sulfide nanowires were deposited on a typical glass substrate. Fig. 5 shows samples of the glass-substrates with nanomaterials deposited on them.

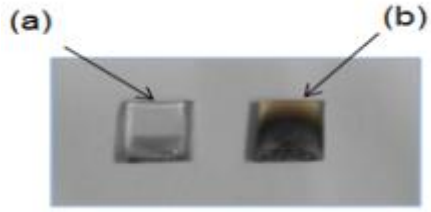

Fig. 5. Samples for glass substrate with (a) nanowires and (b) nanoleaves

1) SEM results: The following figures were the SEM micrographs and measurements made for the nanowires and nanoleaves deposited on glass substrates. On the basis of these micrographs, it was observed that the bismuth sulfide sample A belonged to the category of nanowires.

It was observed that the density of nanowires deposited on the glass substrates were not the same for each of the samples. Since, the curvature made on the fused silica tube during the-dent-process was also varying in location. As well as the substrate placed at zone 2, that might be able for nanowires of different length to be deposited on the glass substrate. The same observations were obtained with nanoleaves.

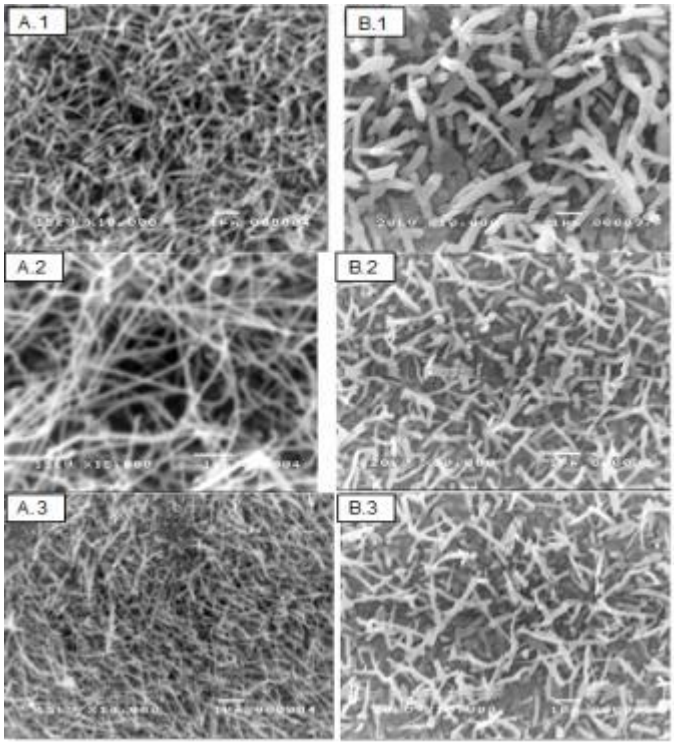

Fig. 6. Micrographs of nanowires---A.1, A.2, A.3, zone 2; and nanoleaves---B.1, B.2, B.3, zone 3, grown at the optimum parameters.

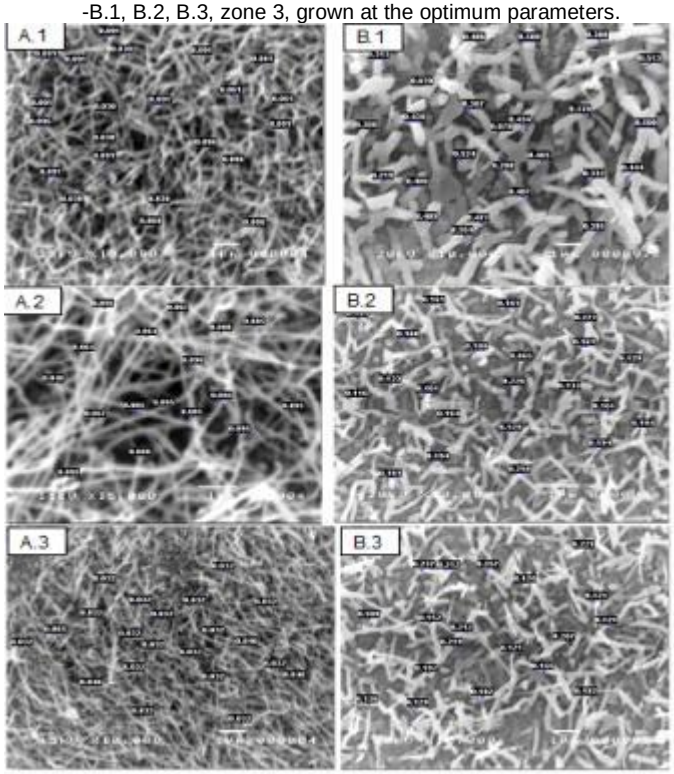

Fig. 7. Micrographs with measurements of nanowires---A.1, A.2, A.3, zone 2; and nanoleaves---B.1, B.2, B.3, zone 3.

2) Elemental composition results: The EDX spectra shown in Fig. 8 below are the representative for nanowires and nanoleaves.

These EDX spectra indicated that the nanowires as well as nanoleaves were indeed comprises with Bismuth Sulfide.

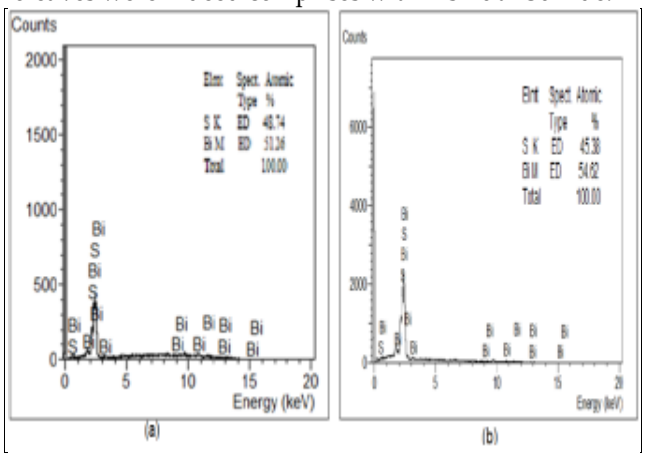

Fig. 8. EDX spectra of Bi_2S_3 (a) nanowires (b) nanoleaves including the elemental composition

3) Quantum Confinement Effect: Photoluminescence of Bi_2S_3 Nanowires (zone 2) and Nanoleaves (zone 3) at parameters: 1200 degree, 4 hours, 60 minutes, which refers to the growth temperature, growth time and ramp time respectively, confirmed that there were blue shift occurring as the nanomaterials decreased in size as shown in fig. 9. This implied that the nanowires were better to use than the larger nanostructures in optical devices.

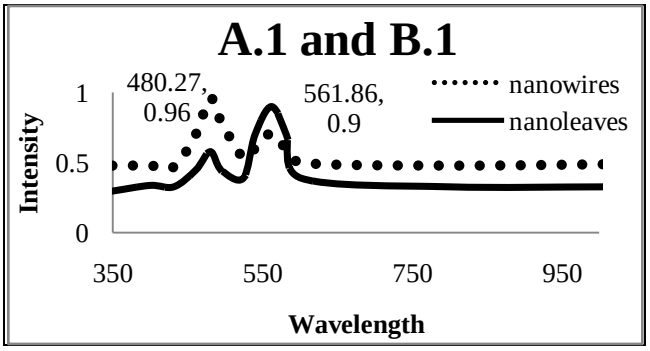

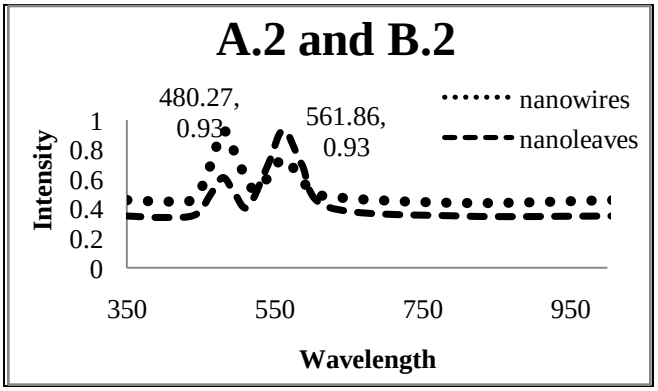

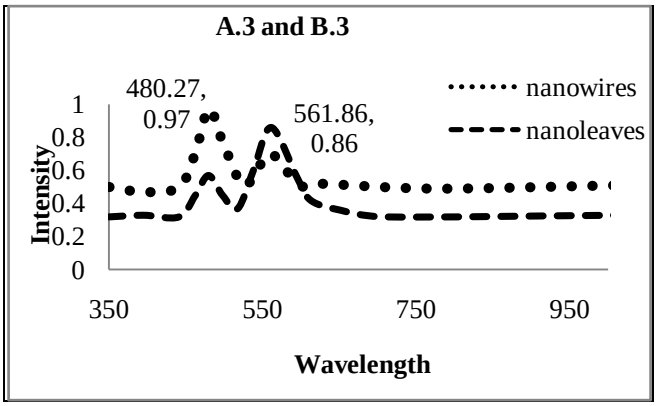

Fig. 9. Normalized PL spectra of Bi_2S_3 nanowires and nanoleaves: A.1, A.2, A.3 and B.1, B.2, B.3 respectively.

TABLE II
CALCULATED ENERGY BAND GAP

Samples		Zone	Peak Wavelength (nm)	Peak Intensity (a.u.)	Energy Gap (eV)
Bi_2S_3 Nanowires	A.1	2	480.27	0.96	2.58
	A.2		480.27	0.93	2.58
	A.3		480.27	0.97	2.58
Bi_2S_3 Nanoleaves	B.1	3	561.86	0.90	2.21
	B.2		561.86	0.93	2.21
	B.3		561.86	0.86	2.21

The calculated energy gap was shown on the Table II. It was from there that the Quantum confinement was observed particularly in terms of band gap from 1.3 eV, 2.21 eV to 2.58 eV for bulk, nanoleaves, and nanowires forms of bismuth sulfide respectively (see appendix C for sample calculation). Furthermore, in all of the samples, almost, the peak intensity of the nanowires was always higher than that of nanoleaves. This could be due to shape effect thus to surface area. In this case nanowires had the larger surface area compared to nanoleaves which means it allows more electrons and holes to return to ground state via optically radiative recombination routes that resulted to high PL intensity.

4) Light-detection demonstration and Voltage-time spectra: The light detection experiment was conducted. At 20 V bias, the following on and off light detection shown by response-time spectra measured on the load resistor under white light was generated.

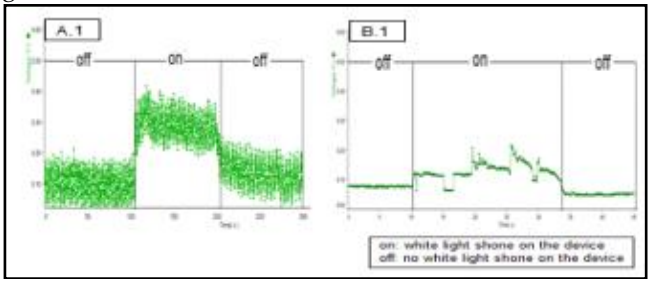

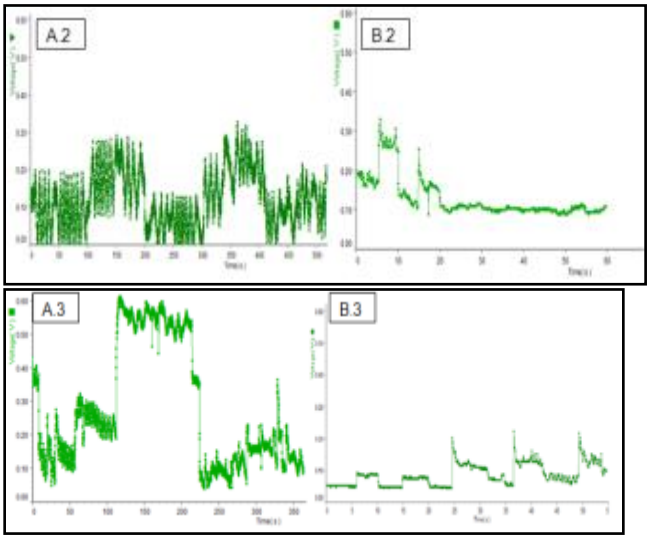

Fig. 10. Response time spectra measured on the load resistor under the white light for Bi_2S_3 nanowires and nanoleaves: A.1, A.2, A.3 and B.1, B.2, B.3 respectively.

TABLE III
Maximum Voltages of the Samples

Samples		Zone	Maximum Voltage (V)
Bi_2S_3 Nanowires	A.1	2	0.41
	A.2		0.33
	A.3		0.61
Bi_2S_3 Nanoleaves	B.1	3	0.22
	B.2		0.33
	B.3		0.22

In this part, it was successfully demonstrated that the bismuth sulfide nanowires can detect light in an ambient environment. It was observed that nanowires had the higher voltage reading dissipated on the load resistor when light shone on it with similar fluctuations to the light source intensity profile (see Appendix B) compared to nanoleaves based on fig. 10 and Table III. But there were also fluctuations observed even the light source was turn off and these might be due to the noise coming from the lighted building and houses surrounding STRC laboratory. Aside from that it was also observed that almost both had fast response when light was shone on them based on the voltage spectra which were similar to the ZnS nanobelts by Zheng et al, (2010).Accordingly, this could be explained by oxygen chemisorption as it played a central role in regulating the dark conductivity under "off" state and the photoconductivity under "on" state for nanowire. A few free electrons in the interior resulted in a low conductivity when the light source was turned off. As the light source was turned on electron-hole pairs was generated in bismuth sulfide nanomaterials and separated by the attraction of the negatively charged ions "O_2^- (ad)", and photon generated holes "h^+" migrate to the surface to recombine with electrons in the ions "O_2^- (ad)". The surplus photon-generated electrons enhance the conductance that resulted to the voltage rise progress. There was equilibrium between the generation of electron hole pairs and desorption of oxygen molecules "O_2^- (g)", and the massive photon-generated electrons keep the steady high conductivity state corresponding to "on" state. The moment the light source was turn off, "O_2^- (g)" capture free electrons and adsorb on the Bismuth Sulfide semiconductor surface as "O_2^- (ad)" greatly reduced the conductance of the device. The progress resulted in the voltage decay progress. In darkness rare electrons were left at the oxygen chemisorption equilibrium, therefore the device recovers to the initial "off" state and returns to "on" state.

For the possible explanation for higher voltage reading for nanowires than nanoleaves, quantum confinement effect played a major role on it. Firstly, the nanowires where the electrons were more confined than nanoleaves meant that it is necessarily requiring a higher energy to let the electron hole pair participates in the photoconductivity. As a consequence, more photons with higher frequency within the visible light had been absorbed so that electrons with high energy were been involved in the process of voltage rise progress generating higher voltage reading. Secondly, nanowires had the higher surface to volume ratio compared to nanoleaves, therefore, lots of oxygen exists on the surfaces of the nanowires that would reduced the net carrier's density and increased the depletion width resulting to more effective oxygen adsorption than nanoleaves. Thus, it was a piece of evidence that the bismuth sulfide nanowires can be used as detector for white light and hence as optical switch in optoelectronic devices.

4 CONCLUSIONS

The Horizontal Vapor Phase Growth technique was discovered to be effective and efficient in fabricating nanowires and other nanomaterials. As the growth temperature increases, the size of nanomaterials also increases.

Quantum confinement effect was verified by the blue shift photoluminescence spectra of bismuth sulfide nanowires in terms of the energy band gap from 1.3 eV in bulk form became 2.58eV.

Bismuth sulfide nanowires photosensor (MSM planar structure) was used to detect light. Since absorption of white light is possible only when the band gap of material is in the range of 1.8 eV to 3.1 eV. Therefore, another piece of evidence that quantum confinement effect happened, when the

nanowires detected white light and became more sensitive to it as depicted on the higher voltage reading dissipated on the load resistor compared to nanoleaves. For the fast response, oxygen chemisorption played the central role for the photoconductive property of the material. Therefore, in the nanowires form, bismuth sulfide could then be used as photosensor for optical devices.

ACKNOWLEDGMENT

This work was supported by Department of Science and Technology, University of the East-Manila and Dr. Gil Nonato C. Santos.

REFERENCES

1. Ahire, R.R., Deshpande, N.G., Gudage, Y.G., Sagade, A.A., Chavhan, S.D., Phase, D.M., Sharma, R., (2007). A comparative study of the physical properties of CdS, Bi_2S_3 and composite CdS-Bi_2S_3 thin films for photosensor application. Sensors and Actuators A 140, pp 207-214
2. Callister, W., (2001). Fundamental of Materials Science and Engineering (An Interactive e-txt). John Wiley and Sons, Inc.
3. Chai, D., Yuan, X.S., Yang, B.J., Qian, Y., (2008). A rational route to synthesize Bi_2S_3 nanorods in large scale. Solid State Communications 148, pp. 444-447
4. Chalsani, P., Grego, R., (2008, April). Light Emitting Diodes. CNS Institute for physics teacher. Retrieved February 17, 2010 from http://www.cns.cornell.edu/cipt/labs/lab-index.html.
5. Chen, Y., Kou, H., Jiang, J., Su, Y., (2003). Morphologies of nanostructured bismuth sulfide prepared by different synthesis routes. Materials Chemistry and Physics 82, pp. 1-4
6. Cua, A. and Lau J, (1996). Measurement of the minority carrier lifetime of $Pb_xSn_{1-x}Te$ thin films using the method of photoconductivity. De La Salle University, Physics Department, Thesis.
7. Espulgar, W. (2010). Characterization Of Silver (Ag) Nanomaterials, Synthesized by Horizontal Vapor Phase Crystal (HVPC) Growth Technique for Antimicrobial Purposes. De La Salle University, Master Thesis.
8. George,T., (2006). *Dictionary of Nanotechnology*. India: Anmol Publications Pvt.Ltd.
9. Gilliland, G., (1997). Photoluminescence Spectroscopy of crystalline semiconductors, Materials Science and Engineering R18, 99-400
10. Goetzberger, Adolf., Knobloch, Joachim., Voss, Bernhard., (1998). Crystalline Silicon Solar Cells, John Wiley & Sons Ltd. Page 9-45.
11. Heavens, O.S., (1965). *Optical Properties of Thin Solid Films*. Dover Publications Inc.
12. Heiman, D. (2004). Photoluminescence Spectroscopy. Northeastern University
13. Liu, Z., Xu, D., Liang, J., Lin, W., Yu, W., Qian, Y.,(2005). Low-temperature synthesis and growth mechanism of uniform nanorods of bismuth sulfide. Journal of Solid State Chemistry 178, pp. 950-955
14. Lu, J., Han, Q., Yang, X., Lu, L., Wang, X., (2007). Microwave-assisted synthesis and characterization of 3D flower-like Bi_2S_3 superstructures. Materials Letters 61, pp. 2883-2886
15. Lu, J., Han, Q., Yang, X., Lu, L., Wang, X., (2007). Preparation of Bi_2S_3 nanorods via a hydrothermal approach. Materials Letters 61, pp. 3425-3428
16. Ma, X., Liu, L., Mo, W., Liu, H., Kou, H., Wang, Y., (2007). Surfactant-assisted solvothermal synthesis of Bi_2S_3 nanorods. Journal of Crystal Growth 306, pp. 159-165
17. Medles, M., Benramdane, N., Bouzidi, A., Nakrela, A., Tabet-Derraz, H., Kebbab, Z., Mathieu, C., Khelifa, B., Desfeux, R., (2006). Optical and electrical properties of Bi_2S_3 films deposited by spray pyrolysis. Thin Solid Films 497, pp 58-64
18. Neaman, D. (2006). *An Introduction to Semiconductor Devices*. New York: McGraw-Hill Companies, Inc.
19. Owens, F. J., and Poole, C. P. Jr. (2008). *The physics and chemistry of nanosolids*. Hoboken, New Jersey: John Wiley & Sons, Inc.
20. Panmand, R.P., Kawade, U.V., Kulkarni M.V., Apte, S.J., Kale B.B., Gosavi, S.W. (2010). Synthesis and characterization of Bi_2S_3 nanocrystals in glass matrix. Materials Science and Engineering B 168, pp. 161-163
21. Parker, Greg., (1994). Introductory Semiconductor Device Physics. Prentice Hall International (UK) Limited. Page143-147
22. Pejova, B., Tanusevski, A., Grozdanov, I., (2005). Photophysics, photoelectrical properties and photoconductivity relaxation dynamics of quantum-sized bismuth(III) sulfide thin films. Journal of Solid State Chemistry 178, pp. 1786-1798
23. Quitaneg, A. (2011). Synthesis and characterization of Cadmium Selenide (CdSe) Quantum Dots Using the Horizontal Vapor Phase Crystal (HVPC) Growth Technique for Sensing Copper Ion Concentrations, De La Salle University. Master Thesis.
24. Shen, X., Yin, Gui., Zhang, W., Xu, Z., (2006). Synthesis and Characterization of Bi_2S_3 faceted nanotube bundles. Solid State Communications 140, pp. 116-119
25. Streetman, B., and Banerjee, S. (2000). *Solid State Electronic Devices*. Prentice Hall, Inc.
26. Thongtem, T., Phuruangrat, A., Wannapop, S., Thongtem, S., (2010). Characterization of Bi_2S_3 with different morphologies synthesized using microwave radiation. Materials Letters 64, pp. 122-124
27. Ubale, A.U., Daryapurkar, A.S., Mankar, R.B., Raut, R.R., Sangawar, V.S., Bhosale, C.H. (2008). Electrical and optical properties of Bi_2S_3 thin films deposited by successive ionic layer adsorption and reaction (SILAR) method. Materials Chemistry and Physics 110, pp. 180-185
28. Wang, D., Shao M., Yu D. (2002). J. Cryst. Growth 243 pp 331
29. Willander, M., Zhao, Q.X., Hu, Q.-H., Klason, P., Kuzmin, V., Al-Hilli ,S.M., Nur, O., Lozovik, Y.E., (2008). Fundamentals and properties of zinc oxide nanostructures: Optical and sensing applications. Superlattices and Microstructures 43, pp. 352-361
30. Willems and van den Wildenberg, (2004). NanoRoadMap project-Work document on Nanomaterials.
31. Winter, M. (1993-2010). WebElements:the periodic table on the WWW. Retrieved Sept 19, 2010 from http://www.webelements.com/compounds/bismuth/dibismuth_trisulphide.html
32. Wu, J., Qin, F., Chan, F.Y.F., Cheng, G., Li, H., Lu, Z., Chen, R., (2010). Fabrication of three-dimensional snowflake-like bismuth sulfide nanostructures by simple refluxing. Materials Letters 64, pp. 287-290
33. Xi, Y., Hu, C., Zhang, X., Zhang, Y., Wang, Z. L., (2009). Optical switches based on Bi_2S_3 nanowires synthesized by molten salt solvent method. Solid State Communications 149, pp. 1894-1896
34. Xu, Y., Ren, Z., Cao, Ren, G., Deng, W.K., Zhong, Y., (2010).A template-free route to prepare Bi_2S_3 nanostructures. Physica B 40, pp. 1353-1358

35. Yu, X., Cao, C., Zhu, H., (2005). Synthesis and photoluminescence properties of Bi_2S_3 nanowires via surfactant micelle template inducing reaction. Solid State Communications 134, pp. 239-243
36. Yu, Y., & Sun, W., (2009). Uniform Bi_2S_3 nanowires: Structure, growth, and field- effect transistors. Materials Letters 63, pp. 1917-1920
37. Young, H. and Freedman, R. (2008). University Physics with Modern Physics 12th edition. Pearson Addison Wesley, Inc.
38. Zhao, W., Zhu, J., Xu, J., Chen, H., (2004). Photochemical synthesis of Bi_2S_3 nanoflowers on an alumina template. Inorganic Chemistry Communications 7, pp. 847-850
39. Zheng, X.J., Chen, Y.Q., Zhang, T., Yang, B., Jiang, C.B., Yuan, B., Zhu, Z. (2010). Photoconductive semiconductor switch based on ZnS nanobelts film. Sensors and Actuators B 147, pp. 442-446.
40. Zheng, X. G., Li, Q. Sh., Zhao, J.P., Chen, D., Zhao, B., Yang, Y.J., Zhang, L.Ch., (2006). Photoconductive ultraviolet detectors based on ZnO films. Applied Surface Science 253, 2264-2267
41. Zhu, G., Liu, P., Zhou, J., Bian, X., Wang, X., Li, J., Chen, B., (2008). Effect of mixed solvent on the morphologies of nanostructured Bi_2S_3 prepared by solvothermal synthesis. Materials Letters 62, pp. 2335-2338
42. Zhu, J.M., Yang, K., Zhu, J.J., Ma, G.B., Zhu, X.H., Zhou, S.H., Liu, Z.G., (2003). The microstructure studies of bismuth sulfide nanorods prepared by sonochemical method. Optical Materials 23, pp. 89-92